RESEARCH ARTICLE

Revealing spatiotemporal travel demand and community structure characteristics with taxi trip data: A case study of New York City

Chen Xie[1,2,3], **Dexin Yu**[1,2,3]*, **Xiaoyu Zheng**[1,2,3], **Zhuorui Wang**[1,2,3], **Zhongtai Jiang**[1,2,3]

1 School of Transportation, Jilin University, Changchun, China, **2** Jilin Research Center for Intelligent Transportation System, Changchun, China, **3** Jilin Province Key Laboratory of Road Traffic, Changchun, China

* yudx@jlu.edu.cn

Citation: Xie C, Yu D, Zheng X, Wang Z, Jiang Z (2021) Revealing spatiotemporal travel demand and community structure characteristics with taxi trip data: A case study of New York City. PLoS ONE 16(11): e0259694. https://doi.org/10.1371/journal.pone.0259694

Editor: Jun Yang, Northeastern University (Shenyang China), CHINA

Received: September 20, 2021

Accepted: October 24, 2021

Published: November 9, 2021

Data Availability Statement: This paper contains information from OpenStreetMap and OpenStreetMap Foundation, which is made available under the Open Database License https://www.openstreetmap.org/copyright. All the data sets are available from the public data set of NYC Open Data https://data.cityofnewyork.us/City-Government/Borough-Boundaries/tqmj-j8zm and New York City Taxi and Limousine Commission (TLC) https://www1.nyc.gov/site/tlc/about/tlc-trip-record-data.page.

Abstract

Urban traffic demand distribution is dynamic in both space and time. A thorough analysis of individuals' travel patterns can effectively reflect the dynamics of a city. This study aims to develop an analytical framework to explore the spatiotemporal traffic demand and the characteristics of the community structure shaped by travel, which is analyzed empirically in New York City. It uses spatial statistics and graph-based approaches to quantify travel behaviors and generate previously unobtainable insights. Specifically, people primarily travel for commuting on weekdays and entertainment on weekends. On weekdays, people tend to arrive in the financial and commercial areas in the morning, and the functions of zones arrived in the evening are more diversified. While on weekends, people are more likely to arrive at parks and department stores during the daytime and theaters at night. These hotspots show positive spatial autocorrelation at a significance level of p = 0.001. In addition, the travel flow at different peak times form relatively stable community structures, we find interesting phenomena through the complex network theory: 1) Every community has a very small number of taxi zones (TZs) with a large number of passengers, and the weighted degree of TZs in the community follows power-law distribution; 2) As the importance of TZs increases, their interaction intensity within the community gradually increases, or increases and then decreases. In other words, the formation of a community is determined by the key TZs with numerous traffic demands, but these TZs may have limited connection with the community in which they are located. The proposed analytical framework and results provide practical insights for urban and transportation planning.

1 Introduction

The city is a large and complex system whose planning and transportation are closely linked to our daily lives. Quantifying the spatiotemporal patterns of residents' travel flow can effectively reflect the dynamics of urban components [1]. Understanding the essence of it can provide us with some perspectives and insights for improving urban planning, transport efficiency, even energy conservation and emission reduction [2].

Funding: Dexin Yu is supported by Jilin Province special Fund for Industrial Innovation (No.2019C024), Jilin Science and Technology Development Project (No.2019010102). The funders had no role in study design, data collection, and analysis, decision to publish, or preparation of the manuscript.

Competing interests: The authors have declared that no competing interests exist.

In the past, the acquisition of residents' travel behaviors was mainly achieved through family travel surveys. The comprehensive information and its collection were labor-intensive and often with short application time and low accuracy [3, 4]. In recent years, there is increasing momentum in the analysis of urban travel through the data collected by travel-related digital sensors. The rapid popularity of high-granularity, multi-source data allows us to extract more accurate travel records and analyze the spatiotemporal mobility characteristics of the flow of people [5]. For example, many cities used smart cards to carry out statistical analyses [6, 7] and predict human travel behavior [8], employed taxi trajectory data to explore travel spatial distribution characteristics [9], and identified travel movement patterns through cell phone data [10]. Similar ideas have also been applied to mining spatiotemporal properties of emerging transportation modes, such as shared cars [11] and electric vehicles [12]. These studies generally found that humans congregate in different geographic locations over time. To further clarified influencing factors and aggregation patterns of travel behavior, many studies introduced spatial statistical models in cities and transport systems and carried out empirical arguments from multiple perspectives. These methods were mainly introduced into the spatial distribution statistical tests of the road network [13], urban bus systems [14], shared bicycles [15], parking [16], and even marine transport demand [17]. However, most of these studies were based on public transportation with fixed routes or short-distance travel, which often could not reflect the characteristics of crowd movement in random travel. The travel pattern of taxis and high-use private cars is more compatible with the city area but rarely appeared in existing studies.

Revealing the spatial pattern of urban traffic through network science does not have a long history. Here we present a brief review. Traditional research usually applied network analysis to street layouts based on urban topology [18]. However, the spatial interpretation of human activities by streets was controversial. Many studies were based solely on network topology methods, such as space syntax [13, 19], which ignored the flow of travel. In recent years, more and more studies divided the transportation system into multiple research units and used network science theory to analyze its flow characteristics and reveal its complex properties. Most research focused on discovering the community structure formed under different modes of transportation, such as revealed the multi-layer unified community structure of private cars, buses, and passengers [20], the evolution characteristics of the community structure of shared bicycle system [2, 15], community distribution of rail transit under different travel ratios [21]. In addition, some studies introduced complex network theory to calculate the clustering coefficient, path length, betweenness centrality in taxi travel networks [22] and confirmed the small-world property [23].

So far, the researches have focused on the illustration of spatial structures formed by different modes of transport, without revealing in depth the internal mechanism and the hidden characteristics of these structures. Past research carried out demonstrations based on the public system constrained by fixed stops, but the spatiotemporal characteristics of random travel behavior were not clear enough. This study fills these gaps and aims to develop a travel analysis framework with an empirical analysis in New York City. In this framework, kernel density estimation is used to discover the spatial hotspots where people depart and arrive. The global and local Moran's I measure the spatial autocorrelation and cluster characteristics of traffic demand. Community detection extracts the network structures of travel. Based on network science, we analyze the weighted degree distribution of communities, the interaction property, and the similarities under different peak periods between the communities, which provide practical insights for urban and transportation planning.

The rest of the paper is organized as follows. In Section 2, we briefly describe the data sets and the division of analytical units. In Section 3, we introduce the overall logical framework and methodology of travel hotspots recognition, spatial autocorrelation, and community characteristics. In Section 4, we provide a case study based on New York City traffic network. In Section 5, we give a discussion of the results. In Section 6, we provide concluding remarks of the paper.

2 Study area and data

2.1 Study area

New York City (NYC) is located in New York State, which is the most populous city in the United States. It is composed of five boroughs——Manhattan, Queens, Brooklyn, Bronx, and Staten Island (Fig 1). So far, taxicabs come in two varieties in NYC, yellow taxis can carry passengers in any city area, green taxis were launched in 2013 to solve the problem of lack of taxi services outside the downtown area. A full analysis of travel patterns at the city level requires the consideration of these two types. Based on taxi flow in the city, this study analyzes the spatiotemporal distribution of travel demand and specifically discusses the potential characteristics of the taxi community structure in NYC based on two varieties of taxi record data.

2.2 Data description and preprocessing

All the data employed in this study is the public data sets of the New York City Taxi and Limousine Commission (TLC) trip record data, including yellow, green taxis, and for-hire vehicle trip records in five boroughs of NYC, which contains the information of ID, pick-up and drop-off time stamp, coordinate, passenger count, trip distance and payment. After excluding extreme weather and holidays, we selected all taxi trip records from 2016.06.06 to 2016.6.12 to divide spatiotemporal units. The Isolated Forest algorithm [24] is used to clean data. There are a total of 2,005,334 travel records on weekdays and 775,836 on weekends after excluding the outliers and trips outside the study area.

2.3 Analytical unit division

An analysis of the trip time series is carried out in one-hour units (Fig 2). From 7 am on weekdays, the traffic flow increases strongly, lasting about until 10 am, and evening peak hours are

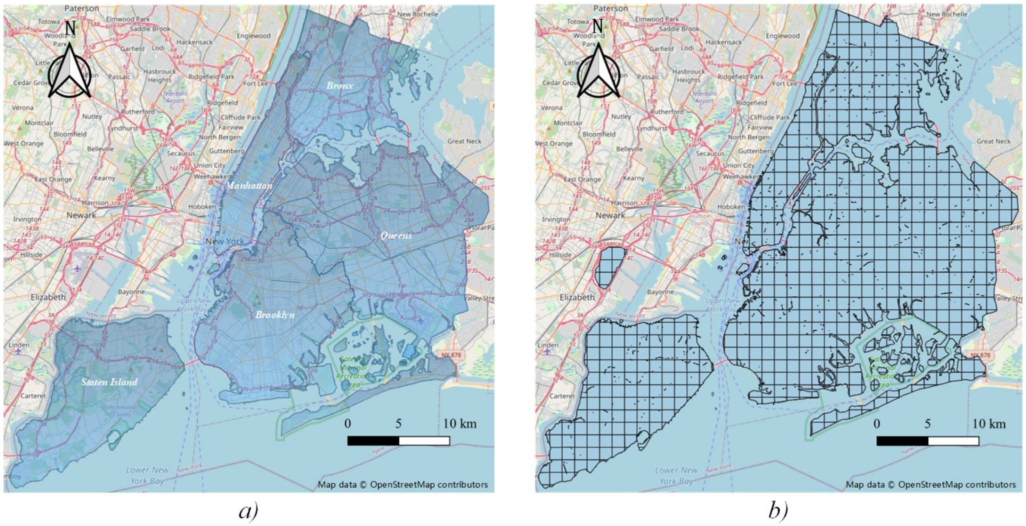

a)

b)

Fig 1. Layout and spatial division of study area.

https://doi.org/10.1371/journal.pone.0259694.g001

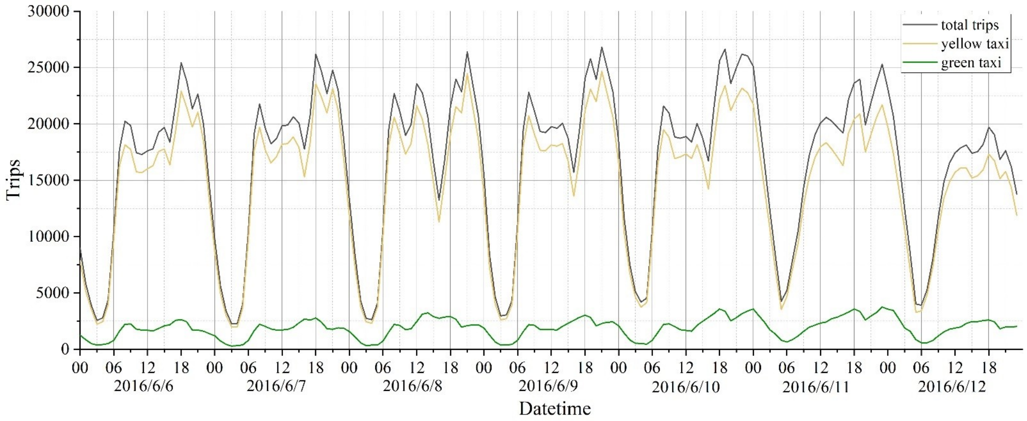

Fig 2. Time series of taxi flow.

https://doi.org/10.1371/journal.pone.0259694.g002

from 5 pm to 8 pm. This feature is reflected in a similar pattern every day of a week. However, the traffic flow on weekends presents different times features. First, there is a small peak time between 12 pm and 3 pm, followed by a more prominent peak time between 5 pm and 8 pm. In addition, there is less traffic on Sunday than on Saturday. In summary, we select Tuesday and Saturday data that are representative and identify four peak periods for the following analysis Table 1.

Most studies selected grid units to group traffic sources and destinations, with sizes ranging from 500 meters to 2 kilometers to detect urban commuting traffic [25]. In our research, we select the size of 1 mile, which represents 25% of the overall trip distance. That is, 75% of the taxi passengers have a travel distance of more than 1 mile, which keeps a lot of information on the movement of taxis between different cells. Finally, 724 spatial analytical units are divided (Fig 1).

3 Methodology

3.1 Logic framework

The overall logic framework of this research is shown in Fig 3, which is divided into 3 parts: data collection and preprocessing, trip spatial distribution pattern modeling, and trip spatio-temporal properties analysis.

3.2 Kernel density estimation

We use kernel density estimation (KDE) to find hotspots in different peak times. KDE is a non-parametric probability density estimation method, which has been used in spatial density analysis of point data [26–28]. If there is a space point *i* with the bandwidth *h*, then the kernel density estimator *D(x,y)* at the center point *(x,y)* is

$$D(x,y) = \frac{1}{nh^2}\sum_{i=1}^{n} K\left(\frac{d_i}{h}\right) \tag{1}$$

where d_i is the distance between the space point and the center point. *K* is the kernel function. The quartic kernel described in Silverman's work is used in this study [29], it is defined by

$$K(u) = \begin{cases} \frac{3}{\pi}(1-u^2)^2,\ if\ 0 < d_i < h \\ 0,\ if\ d_i > h \end{cases} \tag{2}$$

Table 1. Time period definition.

Date	Period	
Tuesday (2016.6.7)	*peak1*	7 am~10 am
	peak2	5 pm~8 pm
Saturday (2016.6.11)	*peak3*	12 pm~3 pm
	peak4	5 pm~8 pm

https://doi.org/10.1371/journal.pone.0259694.t001

In hotspots recognition, the choice of bandwidth h needs to ensure that the OD points on roads are gathered around a plot. According to the area of the plots in this study, we set $h = 300\text{m}$, which can exploit the origin and destination (OD) hotspots based on trip record data from different periods in the urban transportation network effectively and perform spatial visualization analysis.

3.3 Spatial autocorrelation methods

3.3.1 Global autocorrelation. Moran's I index is introduced to explore the potential spatial autocorrelation of traffic demand. Global Moran's I reveals the average degree of correlation between the data in the analysis space and the surrounding area. If there are n spatial units, the global Moran's I of the traffic demand is

$$I = \frac{n}{S_0} \times \frac{\sum_{i=1}^{n}\sum_{j=1}^{n} w_{ij}(x_i - \bar{x})(x_j - \bar{x})}{\sum_{i=1}^{n}(x_i - \bar{x})^2} \tag{3}$$

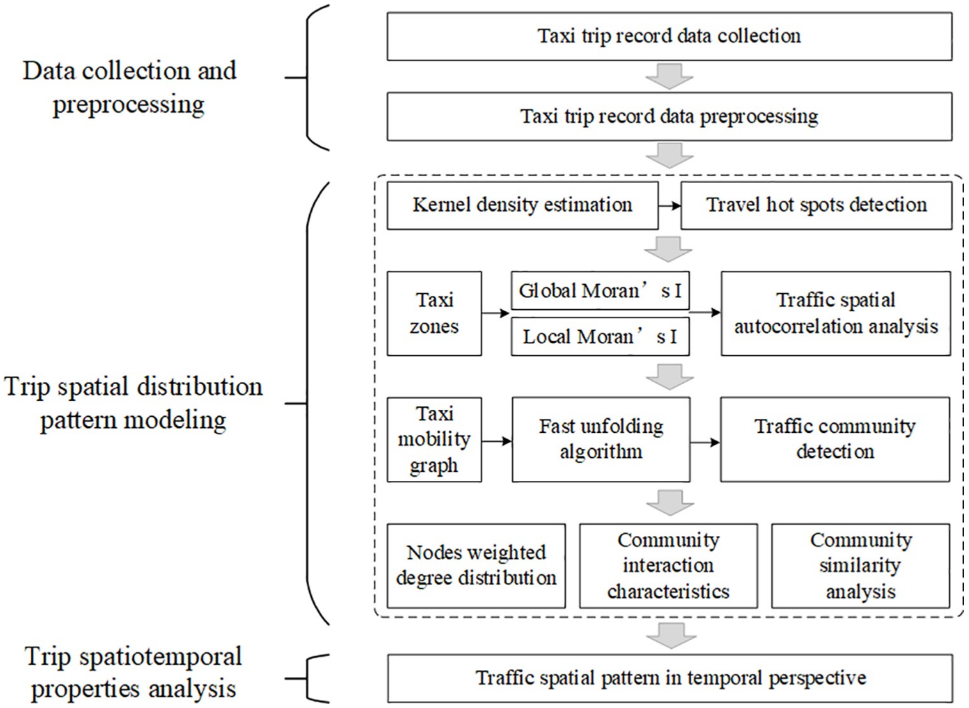
Data collection and preprocessing
Taxi trip record data collection
Taxi trip record data preprocessing
Trip spatial distribution pattern modeling
Kernel density estimation
Travel hot spots detection
Taxi zones
Global Moran's I
Local Moran's I
Traffic spatial autocorrelation analysis
Taxi mobility graph
Fast unfolding algorithm
Traffic community detection
Nodes weighted degree distribution
Community interaction characteristics
Community similarity analysis
Trip spatiotemporal properties analysis
Traffic spatial pattern in temporal perspective

Fig 3. The logic framework of travel spatiotemporal analysis.

https://doi.org/10.1371/journal.pone.0259694.g003

where $S_0 = \sum_{i=1}^{n} \sum_{j=1}^{n} w_{ij}$. x_i and x_j are the value of traffic demand of the cell i and j, respectively. $\bar{x}$ is the average value of global traffic demand. w_{ij} is the spatial weight between i and j, it's defined by $w_{ij} = 1/d_{ij}$, d_{ij} represents the Euclidean distance between the two cells. The Z score is calculated as

$$Z = \frac{I - E(I)}{\sqrt{V(I)}} \tag{4}$$

where $E(I) = -1/(n-1)$, $V(I) = E(I^2)-E(I)^2$, and $I \in [-1,1]$, if I close to 1 with a high Z score indicates great positive spatial autocorrelation, while I close to -1 with low Z score indicates great negative spatial autocorrelation.

3.3.2 Local autocorrelation. The local Moran's I (LISA) [30] calculates an index for each cell in the study area and identifies the specific location and type of correlation in the space. It is calculated by

$$I_i = \frac{Z_i}{S^2} \sum_{j \neq i}^{n} w_{ij} Z_j \tag{5}$$

where $Z_i = x_i - \bar{x}$, $Z_i = x_j - \bar{x}$, $S^2 = \frac{1}{n} \sum (x_i - \bar{x})^2$. The value of the local Moran's I in unit i is determined jointly by two factors: 1) The similarity between unit i and the overall space (Z_i). 2) The similarity between the surrounding areas of unit i and the overall space ($\sum_{j \neq i}^{n} w_{ij} Z_j$). It can be divided into four cases (Fig 4): (a) H-H: High values around neighbors with high values (cluster); (b) L-L: Low values around neighbors with low values(cluster); (c) H-L: High values

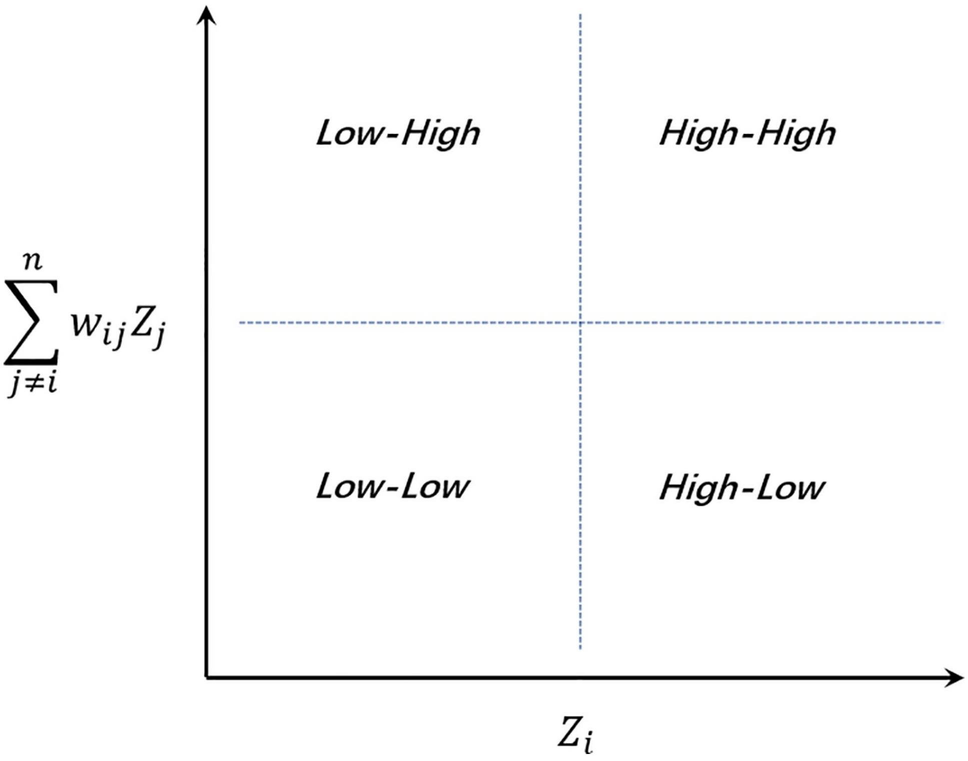

Fig 4. Local Moran's I limit distribution.

https://doi.org/10.1371/journal.pone.0259694.g004

around neighbors with low values(outlier); (d) L-H: Low values around neighbors with high values(outlier).

3.4 Traffic community detection

3.4.1 Taxi mobility graph. Here, we construct a topological structure of multiple research units of the transportation network and map the travel information. An urban mobility system can be represented by a directed graph [15, 20], each cell (mentioned in 2.3) is regarded as a TZ. It can be defined by a directed graph $G = \{V,E\}$ with nodes $V = \{TZ_i|i = 1,2,...n\}$, where n is the number of TZs, and the trips between TZs as edges, denoted as $E = V\times V = \{e_{ij}\}$. For each trip m in the target period T, there is a trip information vector $Trip_m$:

$$Trip_m = \{trip_m^k | trip_m^k = (t_k, x_m^{tk}, y_m^{tk}),\ k = 1, 2,\ t_1 \in T\} \tag{6}$$

where k is an index, 1 for origin and 2 for destination. A trip m at time t includes origin and destination spatiotemporal information $(t_1,\ x_m^{t1},\ y_m^{t1}),\ (t_2,\ x_m^{t2},\ y_m^{t2})$, respectively. If a coordinate $(x_m^{tk},\ y_m^{tk})$ falls inside the TZ_i, then there is $(x_m^{tk},\ y_m^{tk}) \in TZ_i$. Next, an OD matrix is represented by

$$OD = \begin{bmatrix} od_{11} & od_{12} & \cdots & od_{1n} \\ od_{21} & \ddots & & od_{2n} \\ \vdots & & & \vdots \\ od_{n1} & od_{n2} & \cdots & od_{nn} \end{bmatrix} \tag{7}$$

Furthermore, we set the number of passengers as the edge weight W between origin and destination TZs, which denoted as $W = V\times V = \{w_{ij}|w_{ij} = od_{ij}+od_{ji}\}$.

3.4.2 Fast unfolding algorithm. The community detection algorithm divides the network into sub-groups with tight internal connections between nodes, consisting primarily of three categories: division, cohesion, and optimization methods. The last depends on the solution of the objective functions without defining parameters artificially. Therefore, we choose the Fast unfolding algorithm [31] to reveal the community structures of the urban traffic network. It aims to maximize the modularity, for a weighted traffic network, the modularity is defined as

$$\begin{gathered} Q = \frac{1}{2m}\sum_{i,j}\left[w_{ij} - \frac{k_i k_j}{2m}\right]\delta(C_i, C_j) \\ \delta(a, b) = \begin{cases} 1 & when\ \text{a} \quad == \quad \text{b} \\ 0 & \text{otherwise} \end{cases} \end{gathered} \tag{8}$$

where m is the sum of weights of the network, w_{ij} is the edge weight between TZ_i and TZ_j. k_i, k_j are the sum of weights of edges attached to TZ_i and TZ_j, respectively. Where $k_i = \Sigma_j w_{ij}$, $k_j = \Sigma_i w_{ji}$. C_i is the community to where TZ_i is assigned. At the first stage, the algorithm calculates the modularity gain ΔQ by moving an isolated TZ_i into a community

$$\Delta Q = \left[\frac{\sum_{in} + 2k_{i,in}}{2m} - \left(\frac{\sum_{tot} + k_i}{2m}\right)^2\right] - \left[\frac{\sum_{in}}{2m} - \left(\frac{\sum_{tot}}{2m}\right)^2 - \left(\frac{k_i}{2m}\right)^2\right] \tag{9}$$

where Σ_{in} is the sum of edge weights within a community, while Σ_{tot} is the sum of edge weights of all nodes in the community. $k_{i,in}$ denotes the sum of weights of edges originating from TZ_i to nodes in the community. Then the algorithm assigns node TZ_i to the community with the largest ΔQ. At the second stage, it treats the community generated in the previous step as a new node. Iteration until the modularity Q in the network is maximized, thus forming a network community structure with tight internal connections.

3.5 Community structure analysis

3.5.1 Weighted degree and distribution. Based on the complex network theory, we specify several indicators for community structure analysis of TZs. For each peak period, we focus on quantifying the number of passengers between nodes rather than the number of trips. Therefore, the weighted degree [32–34] $deg_w(TZ_i)$ is used to measure the importance of the node TZ_i, which is defined by

$$\deg(TZ_i)_{in} = \sum\nolimits_i e_{ij} \tag{10}$$

$$\deg(TZ_i)_{out} = \sum\nolimits_j e_{ij} \tag{11}$$

$$\deg(TZ_i) = \deg(TZ_i)_{in} + \deg(TZ_i)_{out} \tag{12}$$

$$\deg_w(TZ_i) = \sum\nolimits_{\deg(TZ_i)} w_{ij} \tag{13}$$

where $deg(TZ_i)_{in}$ and $deg(TZ_i)_{out}$ are the in-degree and out-degree of node TZ_i, respectively [34]. According to the definition of degree distribution [35], we introduce the idea of weighted degree distribution with the probability distribution of the weighted degree of TZs in the traffic network.

$$\mathrm{P}_k(I) = \frac{N_k(I)}{N_k} \tag{14}$$

If the set of $Community = \{C_k|k = 1,2,\ldots m\}$, $\mathrm{P}_k(I)$ is defined as the fraction of nodes in a community network C_k with a weighted degree within a numerical interval I. N_k is the number of nodes in the community C_k, $N_k(I)$ is the number of nodes in the community C_k which nodes' weighted degree falls in I.

3.5.2 Interaction intensity. In the analysis of community interaction characteristics, we propose to use the edge weight and weighted degree of nodes [34] to quantify the intensity of node-community interactions. For a node TZ_i, its interaction intensity S_i with community C_k is calculated by

$$S_{i,k} = \frac{\sum_j w_{ij}}{\deg_w(TZ_i)} (TZ_j \in \mathrm{C}_k) \tag{15}$$

It can be understood as if TZ_i and TZ_j are in the same community, $S_{i,k}$ measures the intensity of interaction with the community where TZ_i is located, otherwise, it measures the intensity of interaction with other communities. For each TZ_i, there is $\sum_{k=1}^{m} S_{i,k} = 1$.

3.5.3 Similarity index. M. Yildirimoglu et al propose a similarity measurement of different transport network communities (bus network, passenger network, and car network) [20]. Based on this method, we introduce the similarity index of the traffic network community at different time periods. It is calculated by

$$\begin{gathered} \sigma_{uv} = \frac{\sum_i \sum_{i\neq j} \alpha_{ij}^u \times \alpha_{ij}^v}{\min(\sum_i \sum_{i\neq j} \alpha_{ij}^u, \sum_i \sum_{i\neq j} \alpha_{ij}^v)} \\ \alpha_{ij}^u = \begin{cases} 1 & \text{if } i \text{ and } j \text{ are in the same community in time period } u \\ 0 & \text{otherwise} \end{cases} \end{gathered} \tag{16}$$

where *u* and *v* are different time periods, respectively. It measures the proportion of node pairs that are consistently allocated to the same community at different periods, where $\sigma_{uv} \in [0,1]$. The numerator represents the number of OD pairs that are consistently assigned to the same community over the two periods. If an OD pair od_{ij} falls in the same community in the period *u* and *v*, there is $\sigma_{ij}^u \times \sigma_{ij}^v = 1$.

4 Case study results

The OD flow map of each time period is shown in Fig 5, with more obvious edges as the weight increases. Travel flows are mainly distributed in the surroundings of Manhattan and distant transportation hubs.

4.1 Hotspots detection

The KDE method in ArcGIS is used to extract the hotspots from taxi OD points. A grid of 50m, *h* = 300 is selected for detailed visualization, and we use the natural break method to show the results (Figs 6 and 7). Manhattan is the most important financial and commercial district of NYC, with multiple transportation hubs. The high density of roads and the multiple land use functions make the most of trips originate from this area. On weekday, *peak1* origin demand (Fig 6A) is mainly concentrated in central Manhattan, widely distributed in the transportation hubs of the bus (Port Authority Bus Terminal), subway (Penn Station, Grand Central Terminal), and airport (LaGuardia Airport). Destination hotspots are concentrated in central and southern Manhattan, including the Grand Central Terminal and the surroundings of Park Avenue, with many commercial sites around it (Fig 6B). Moreover, the World Trade Center surrounding areas and the southern financial districts of Manhattan with light traffic concentrations (Fig 6B). At this time period, transportation is mainly used for commuting. We also find that the multiple medical sites on the Upper East Side and south of York Avenue have a slightly high concentration of traffic.

Taxi origin hotspots during *peak2* on weekday are mainly distributed at Penn Metro Station, Central Station, Park Avenue, 57th Street, East 86th Street, and LaGuardia Airport (Fig 6C). The southern part of the Park Avenue hotspot is a commercial area, while the northern part of Park Avenue, 57th Street, and Madison Avenue include a large number of catering facilities. Moreover, the East 86th Street hot zone, which includes banks and schools also shows a slight concentration. Destination hotspots are widely distributed, including land use for residential, catering, shopping, entertainment (Fig 6D). It can be inferred that some people do not return home directly after work, but engage in a series of other activities.

The taxi origin hotspots during *peak3* on weekends are also widely distributed in large public transportation hubs, like Penn Station, Grand Central Terminal, Port Authority Bus Terminal, and LaGuardia Airport (Fig 7A). Unlike weekdays, the department stores (Bergdorf Goodman, Bloomingdale), parks (Central Park, Union Square), and land use of worship (St. Patrick's Cathedral) appear from the results. In addition to the places mentioned above,

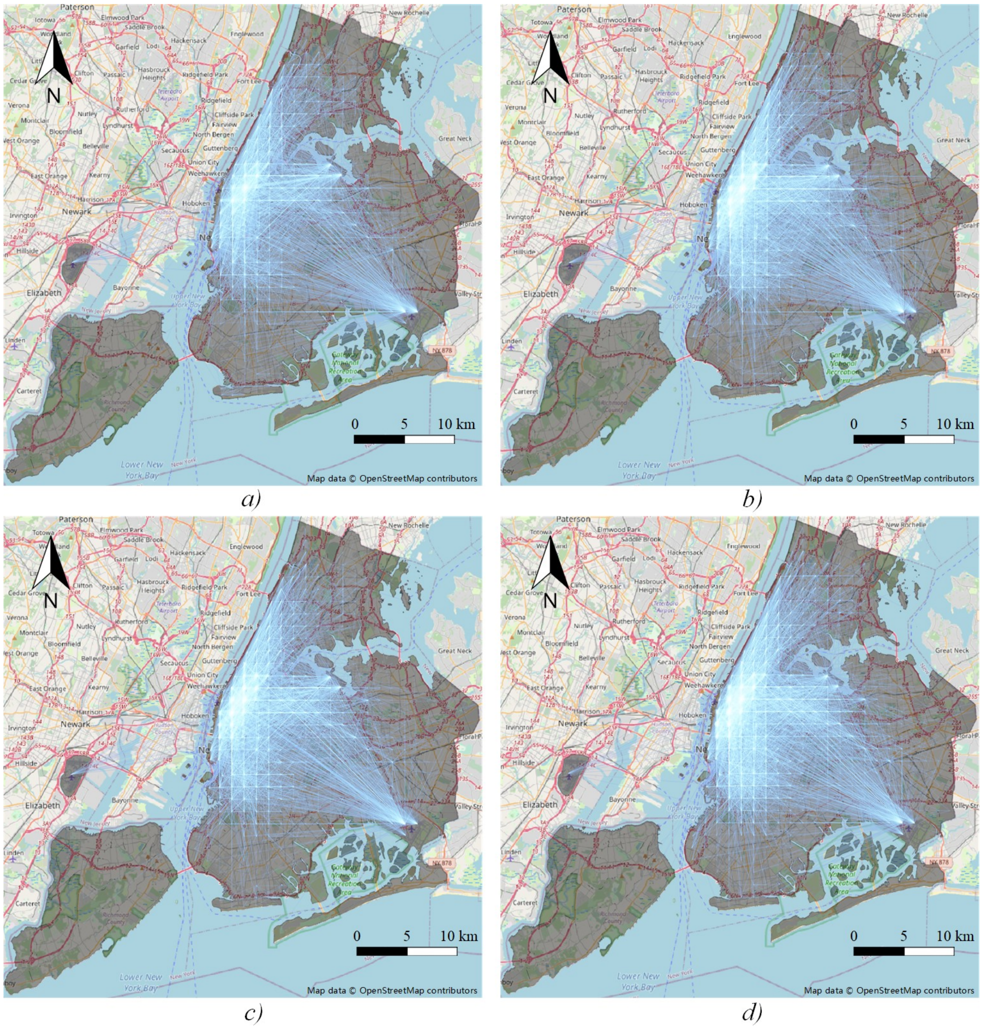

a)

b)

c)

d)

Fig 5. OD flow map. a) *peak1*; b) *peak2*; c) *peak3*; d) *peak4*.

https://doi.org/10.1371/journal.pone.0259694.g005

people also tend to get off in the surroundings of Broadway (Fig 7B), which located in many theaters. In general, people travel mainly for entertainment and socializing during this time.

The taxi origin hotspots of *peak4* and *peak3* are roughly the same. However, Meatpacking District is the unique origin hotspot of *peak4* (Fig 7C), where located American art museum, well-known clothing stores, and elevated parks. The destination hotspots in *peak4* still include department stores and parks but are more focused on Broadway (Fig 7D). It can be inferred that when traveling for entertainment, people tend to arrive at parks and department stores during the daytime and go to theaters at night.

4.2 Spatial autocorrelation analysis

Under the significance level of p = 0.001, the global Moran's I and Z-score of each peak period are shown in Table 2.

The global Moran's I in each period is positive and close to 1 with high Z scores, so traffic demand presents a significant clustering pattern during all peak times with a spatially positive correlation characteristic (Table 2). Furthermore, since the crowds are densely concentrated

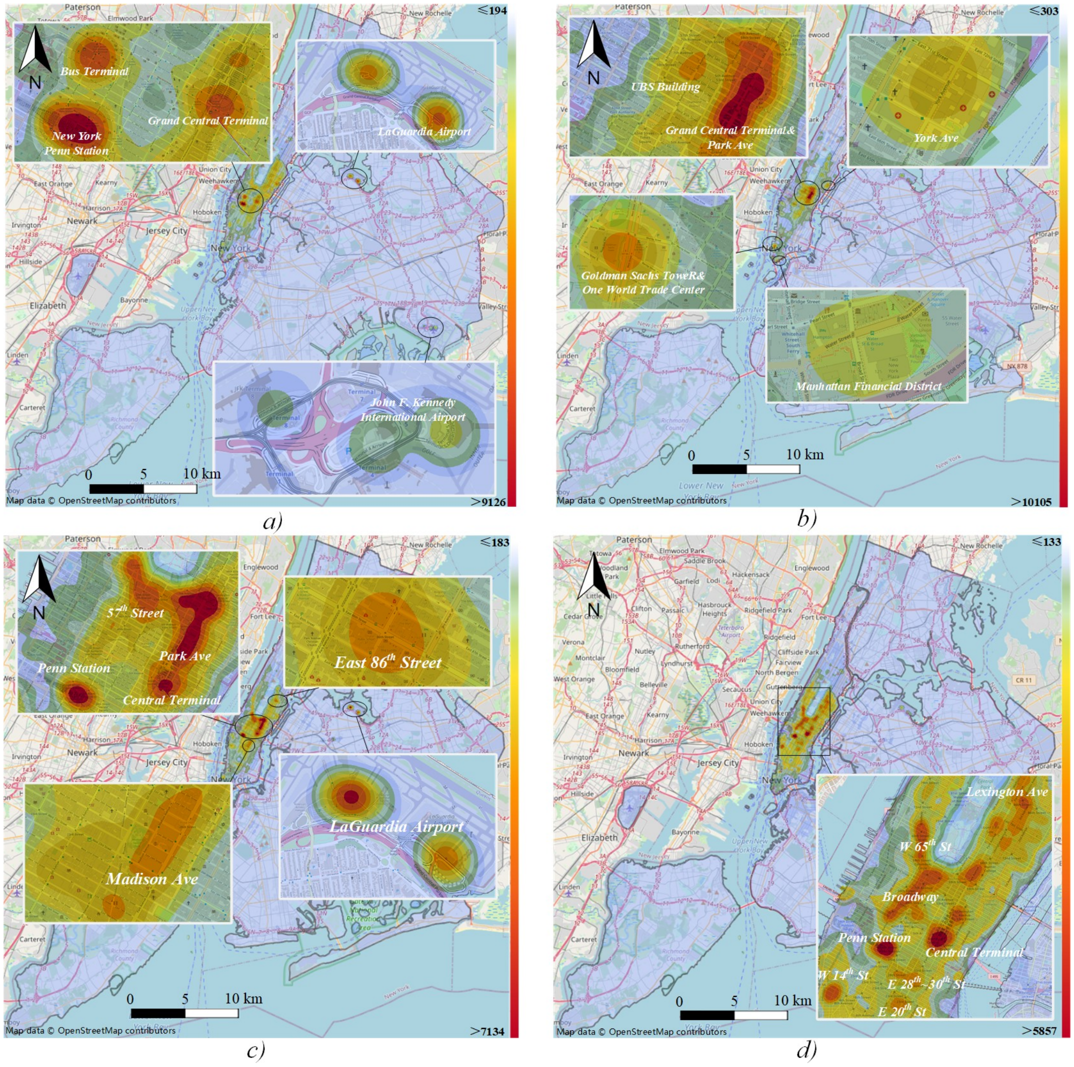

Fig 6. Hotspots of *peak1* and *peak2*. a) *peak1* origin; b) *peak1* destination; c) *peak2* origin; d) *peak2* destination.

https://doi.org/10.1371/journal.pone.0259694.g006

near Broadway during *peak4*, the spatial autocorrelation is higher than in other periods. The local Moran's I pattern and statistical significance of trip volume with two subgraphs in each peak time are shown in Figs 8 and 9.

The traffic demand in the central area of Manhattan in NYC shows the characteristics of the H-H cluster in all periods. For origin demand during *peak1*, the most significant positive correlation area includes Penn Station with a level of p = 0.001 and then gradually decreases in surrounding areas (Fig 8A). While for the destination, the Grand Central Terminal and surrounding areas of Park Avenue have the highest level of significance, and also exist in southern Manhattan (Fig 9A). In other words, there is a tendency for passengers to travel south generally.

At the significance level of p = 0.001, *peak4* shows a significant positive correlation in the southern part of Central Park (origin demand), Union Park, Broadway, and transportation hubs (destination demand). We can see that taxis also have a southward flow trend (Figs 8D and 9D). In addition, traffic demand during every peak period has L-H clustering in the Queens-Midtown tunnel area, while passenger arrivals show L-L clustering in the east of NYC

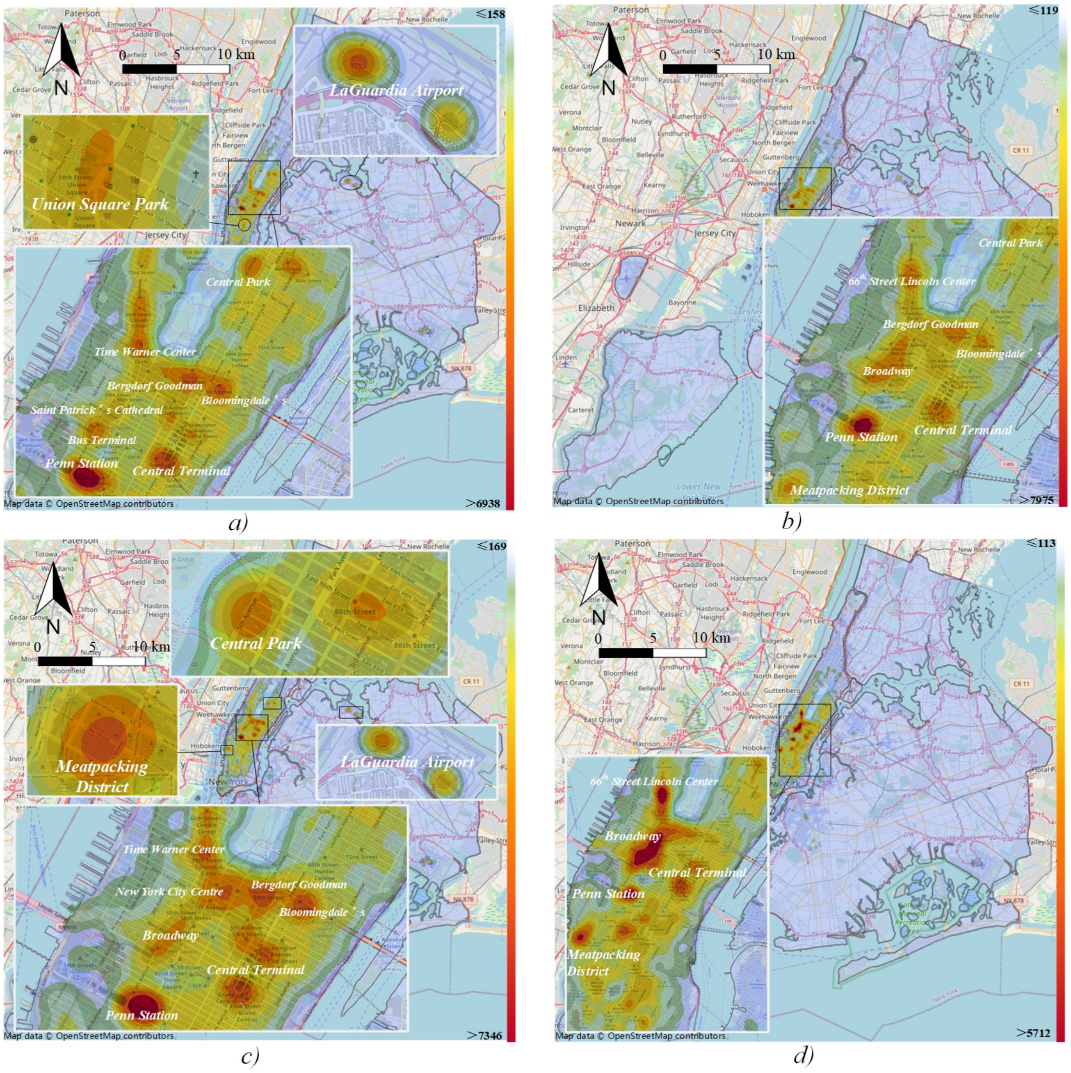

Fig 7. Hotspots of *peak3* and *peak4*. a) *peak3* origin; b) *peak3* destination; c) *peak4* origin; d) *peak4* destination.

https://doi.org/10.1371/journal.pone.0259694.g007

(Fig 9). The spatial distribution of taxi destinations is wider than origin. It can be inferred that taxis tend to carry passengers in the central area of Manhattan and drive them to the far peripheries.

Table 2. Results of global Moran's I.

Type	Period	Global Moran's I	Z-score
origin	*peak1*	0.729	15.580
	peak2	0.690	15.460
	peak3	0.737	16.041
	peak4	0.747	16.357
destination	*peak1*	0.598	16.137
	peak2	0.752	16. 052
	peak3	0.758	19.521
	peak4	0.779	20.755

https://doi.org/10.1371/journal.pone.0259694.t002

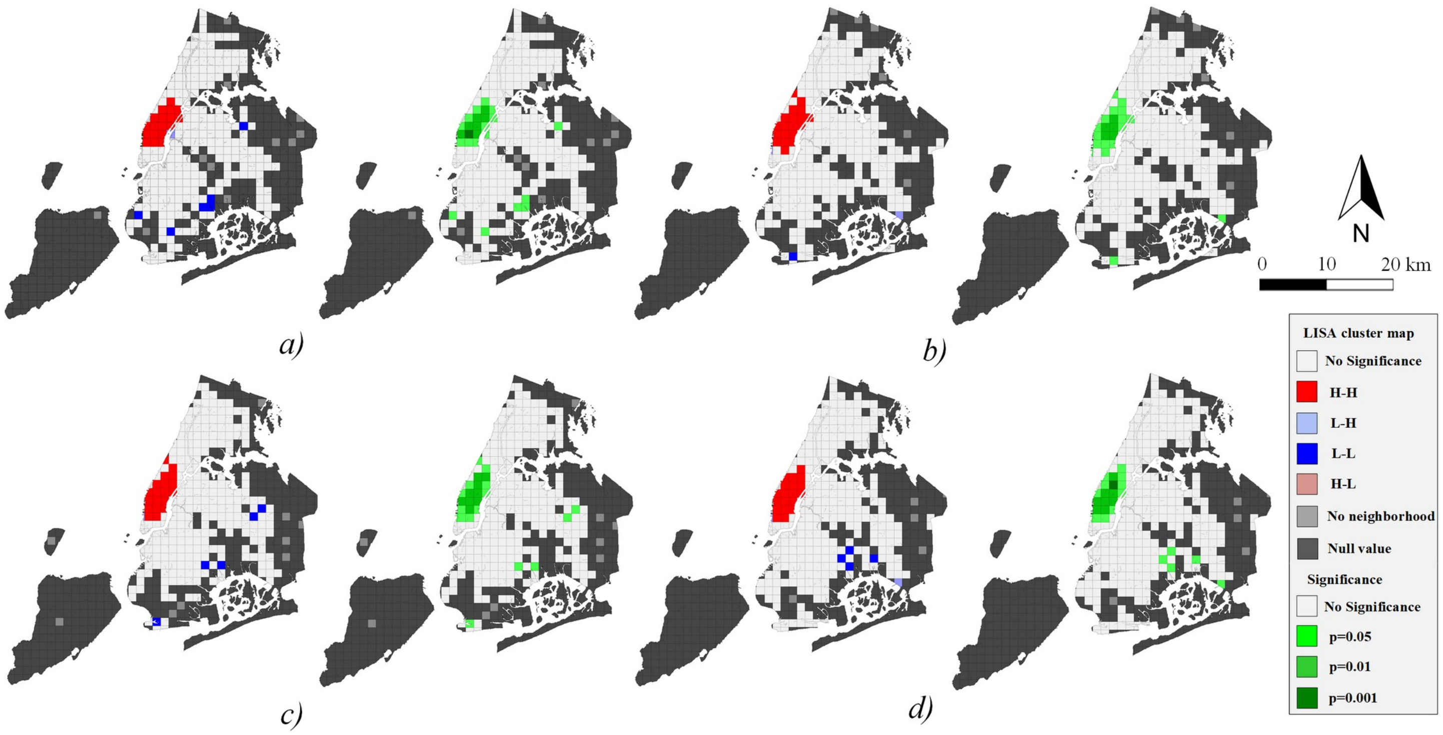

Fig 8. Spatial autocorrelation of origin demand. a) *peak1*; b) *peak2*; c) *peak3*; d) *peak4*.

https://doi.org/10.1371/journal.pone.0259694.g008

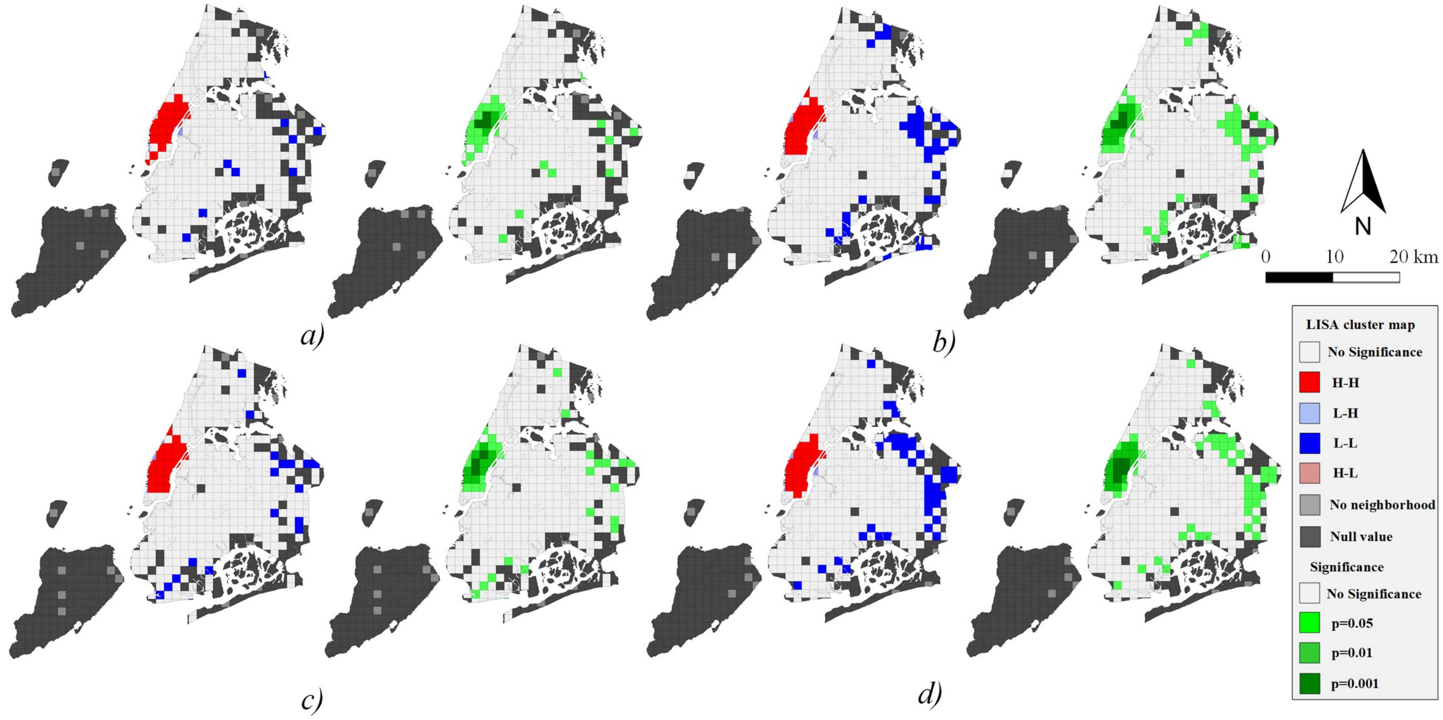

Fig 9. Spatial autocorrelation of destination demand. a) *peak1*; b) *peak2*; c) *peak3*; d) *peak4*.

https://doi.org/10.1371/journal.pone.0259694.g009

4.3 Community structure analysis

Fig 10 shows the community structures (the background of the network means no trip connected) during each peak period. The OD pairs within a community are densely communicated via taxi flow. Specifically, south Manhattan always forms a separate community, whereas Brooklyn and Queens are sometimes connected. During *peak3*, there is a special community that is geographically dispersed, probably because the connection between transportation hubs that fall into TZs is closer than in other periods (Fig 10C). In general, the community layout is similar to the boroughs distribution of NYC, where areas separated by the sea are often divided into different communities.

Information on nodes and weights of communities is shown in Table 3. Due to the idea of the Fast unfolding algorithm, the communities often have the largest edge weights within the community and are weakly connected to other communities.

Based on traffic communities, we reveal the weighted degree distribution characteristics of each community. We focus on the weighted degree of the network because it can better reflect the travel behavior of individuals in the urban transportation system rather than the degree of

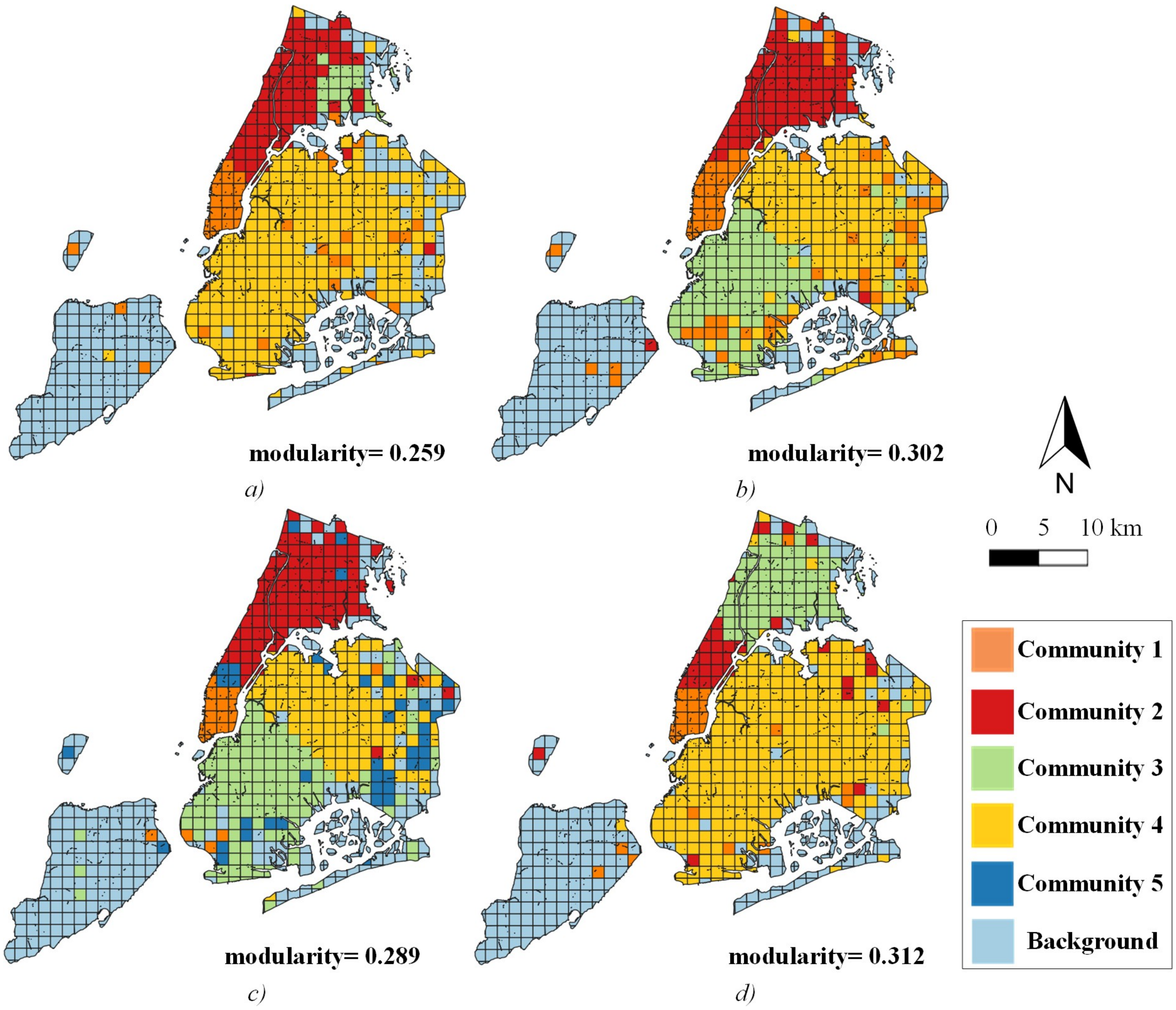

Fig 10. Traffic network community structures. a) *peak1*; b) *peak2*; c) *peak3*; d) *peak4*.

https://doi.org/10.1371/journal.pone.0259694.g010

Table 3. Nodes and weights information of communities.

Period	C_k	1	2	3	4		$\Sigma_k w_{ij}$
Peak1	1	35993	20440	14	3282		59729
	2	-	20609	73	1021		21703
	3	-	-	93	5		98
	4	-	-	-	4196		4196
	nodes	44	74	17	250		85726
Peak2	C_k	1	2	3	4		$\Sigma_k w_{ij}$
	1	70338	13733	2980	2667		89718
	2	-	8489	87	379		8955
	3	-	-	3706	473		4179
	4	-	-	-	3177		3177
	nodes	76	82	103	156		106029
Peak3	C_k	1	2	3	4	5	$\Sigma_k w_{ij}$
	1	22031	7686	1599	358	15250	46924
	2	-	17639	297	441	12094	30471
	3	-	-	3813	298	890	5001
	4	-	-	-	2389	684	3073
	5	-	-	-	-	8070	8070
	nodes	24	94	126	108	41	93539
Peak4	C_k	1	2	3	4		$\Sigma_k w_{ij}$
	1	25796	24281	394	3846		54317
	2	-	34185	3216	3330		40731
	3	-	-	2236	291		2527
	4	-	-	-	11304		11304
	nodes	27	36	72	273		108879

https://doi.org/10.1371/journal.pone.0259694.t003

TZs. Given the small number of nodes and the large weighted degree discrepancy of communities, we set a numerical interval *I* for statistics of each community.

According to the analytical snapshot (Fig 11), the weighted degree of a few TZs is much larger than that of the majority TZs. Furthermore, their weighted degree follows the power-law distribution from a community perspective, that is, $P(I) \sim I^{-\gamma}$. The R-square of each fitted curve exceeds 0.9 (except community3 in *peak1*), which indicates every community during the rush hours has at least one TZ that has a strong impact on passenger attraction or departure. This is often a precondition for the formation of a tightly connected transport community.

Fig 12 shows the results of the interactive features of communities in each peak period. The abscissa represents the weighted degree of nodes located in the community, and the ordinate is the interaction intensity index. Each row represents a period, while a subgraph in a row represents the interaction intensity between nodes in a community and other communities during this period. For example, the first subgraph in Fig 12A means the relationship between the weighted degree of nodes in community 1 and the interaction intensity between communities 1 ~ 4 during *peak1*, which is marked with triangles of different colors. Under the overall observation, we can see that as the weighted degree of nodes increases, their interaction intensity within the community always tends to increase, especially when the weighted degree of nodes is situated before the median current. Furthermore, as the weighted degree increases to a certain extent, the intensity of the interaction stabilizes or decreases. It can be understood that the extremely significant or insignificant nodes in most communities often have limited contact with the community in which they are located, while some moderately important nodes have

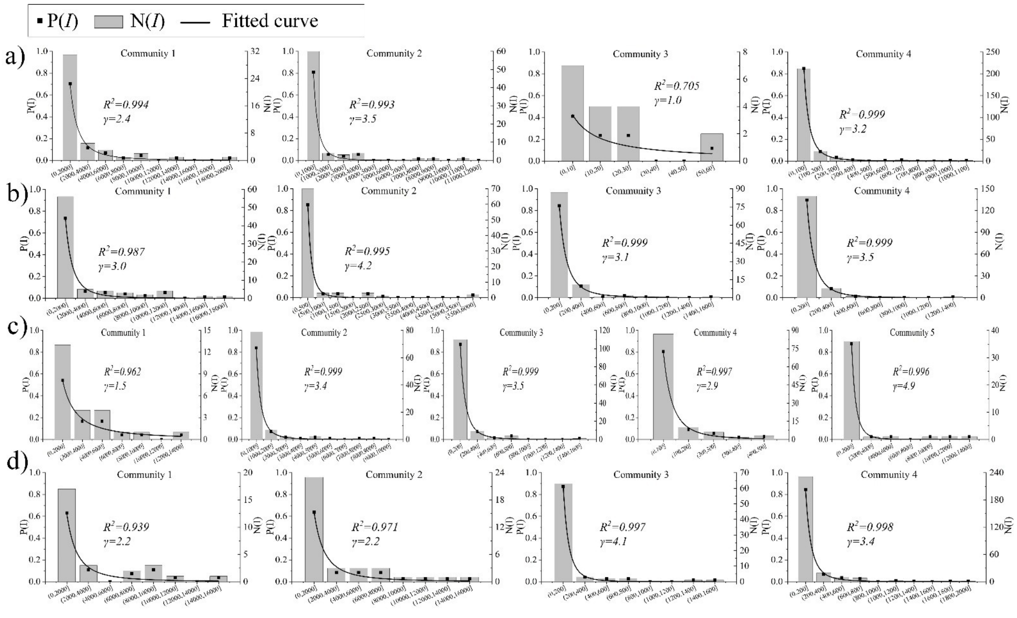

Fig 11. TZs weighted degree distribution. a) *peak1*; b) *peak2*; c) *peak3*; d) *peak4*.

https://doi.org/10.1371/journal.pone.0259694.g011

the highest correlation within the community. On the contrary, as the weighted degree of nodes increases, their interaction intensity with other communities always tends to decline but to increase when great to some extent (Fig 12, subgraph 1, 2, 4 of a), subgraph 2, 3, 4 of b), subgraph 1, 2, 3, 5 of c), d)).

Even if most nodes show the above characteristics, we also find a few particular cases, such as subgraph 3 of a), subgraph 1 of b), and subgraph 4 of c), Fig 12. As the weighted degree of nodes increases, the interaction intensity with the community generally continues to increase, while with other communities continues to decline. This interaction feature is the potential expression of the close relationship between nodes within the community. According to the idea of the Fast unfolding algorithm, the increase of modularity is often reflected in the high connection of nodes within the community and the sparse connection outside. Therefore, this is expected to lead to a better division of the community.

Table 4 shows the similarity results for OD pairs during each peak period. The similarity between communities in each peak period is over 50%. It is worth mentioning that the similarity between *peak3* and *peak4* is slightly higher than in other periods because people's travel purposes are more similar in these two periods, that is, people are more willing to participate in entertainment and social activities on weekends. Overall, traffic community structures are relatively stable over different rush hours.

5 Discussion

5.1 Spatial community structure of taxi trips

Community detection through travel behavior is an effective strategy to discover the underlying structure of cities [1], the formation of communities often signifies the emergence of compact structures in urban areas. Past research ignored the travel flow of people [36] or only stayed on the community structure layout [20]. We quantify the structure characteristics through network theory to fill this gap. As aforementioned, TZs with numerous passengers may have a limited connection with the community in which they are located, but there are a

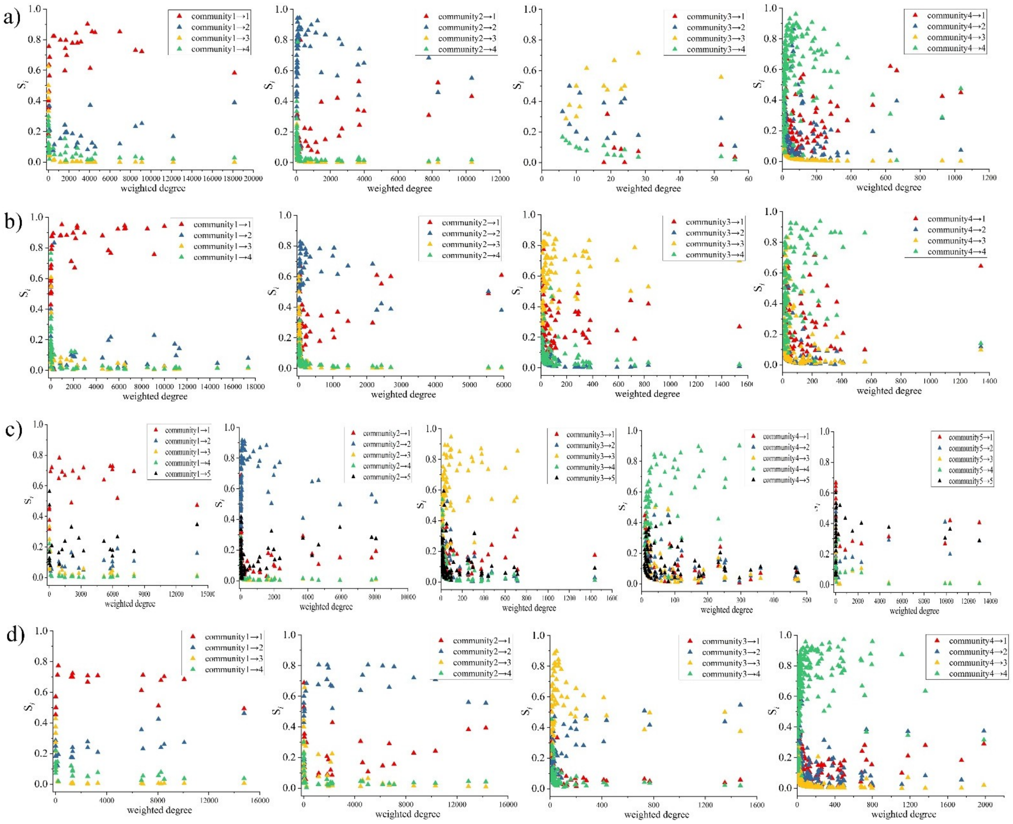

Fig 12. TZs interaction intensity between communities. a) *peak1*; b) *peak2*; c) *peak3*; d) *peak4*.

https://doi.org/10.1371/journal.pone.0259694.g012

few exceptions that some of them in the community still have close internal connections (Fig 12). The latter is encouraging because the structure of the traffic community at its period fits very well with the travel within the community, which is more conducive to the formation of compact development urban areas. Some studies have found that the city's polycentric [37, 38] and compact development [39] is an effective strategy for reducing traffic congestion. Diverse land use in areas ensures that people travel shorter distances and no longer congregate in specific areas of the city [39]. Through the interaction index in communities, we can quickly capture the level of regional interaction of travel flow in key locations and provide some practical insights for the development of compact cities and alleviation of traffic congestion. On the contrary, as the importance of TZs increases, most TZs' interaction intensity with other communities decreases rapidly until it approaches zero (Fig 12). This is because the modularity changes in the Fast unfolding algorithm are often insensitive to OD pairs with small edge weights. It also indicates that most people prefer to travel within the communities.

Table 4. Community structures similarity.

Period	*peak1*	*peak2*	*peak3*	*peak4*
peak1	1	0.521	0.531	0.532
peak2	-	1	0.545	0.524
peak3	-	-	1	0.571
peak4	-	-	-	1

https://doi.org/10.1371/journal.pone.0259694.t004

A well-divided traffic community often has very little external contact. However, the boundary between community 1 and community 2 is often not very clear, that is, the TZs of high importance in community 1 also undertake most of the travel in community 2 and vice versa. According to Fig 10, community 1 is located in southern Manhattan, while community 2 is located in northern and central Manhattan, even in the Bronx. They are very close and without large geographical separation. Moreover, it can be seen that most of the trips in NYC take place inside Manhattan according to Figs 6 and 7. Although they finally meet the algorithm termination in the community dividing process, it is also the main factor that inhibits the increase in modularity. Sun et al. illustrated that the smaller the modularity, the more congested the traffic network [40]. Therefore, in the actual planning of urban traffic and the compact design of the city, we need to focus on this traffic characteristic. It prevents the better division of communities, likely due to the lack of a specific land-use function within the community. The unique land-use function simultaneously attracts trips between multiple communities, leading to a large gathering of vehicles and people.

5.2 Relationship among hotspots, communities and their characteristics

The hotspots of a city can be reflected by the traffic demand, and they globally reveal the critical areas of the entire city. In NYC, they present a cluster distribution layout (Figs 8 and 9). Through the global and local Moran's I, we can discover the statistically significant autocorrelation of traffic hotspots and find the potential geographical location. The presented results are highly consistent with the hotspots found by KDE, which validates the approach in spatial analysis from the taxi mobility network.

Even if there is only one acknowledged central area in NYC (Manhattan), taxi trips at different periods still form an obvious community structure in space (Fig 10). They are relatively stable over time, with nodes within a community generally adjacent geographically. According to the analysis of this study, hotspots in urban areas are often a requirement for the formation of traffic communities (Fig 11). While their interaction within the community is limited, it is more likely to prevent the formation of a better community structure. As for a polycentric and compact urban development, it seems the best approach is to disperse the hotspots and integrate various land functions.

5.3 Potential applications of the framework

Taxi companies may find that the framework of this study is valuable for the identification and prediction of where passengers depart and arrive. It mainly reveals two kinds of information: First, hotspots detection finds the specific location of passengers to ride in different rush hours and identifies the travel destination of people. Capturing the hotspots for passengers in time can provide considerable benefits to taxi companies. Second, the spatial statistical methods reveal the areas where the traffic demand continues to be concentrated, as well as the geographical boundaries with unpopular districts. These hotspots should be given higher priority during the taxi passenger search period.

Urban planners can also get helpful insights from the results. People tend to travel for short distances, so community structure may be formed at any period, while is not ideal enough sometimes. According to the analysis of this study, the reason for preventing a well-division of a community is that some important TZs attract a large number of passengers from other communities, which seems to be due to a lack of required land functions in other communities. Moreover, important TZs can be more decisive in the formation of a community. As a result, a compact and polycentric urban development seems to disperse these key TZs geographically and is equipped with perfect urban functions to alleviate the traffic congestion caused by passenger gathering. The interaction intensity can be used to assess the level of compaction of a city. For example, urban planners can capture the key areas that inhibit the compact development in the city by judging their interaction intensity between the communities and plan for better urban areas by exploiting the land use functions.

6 Conclusion

This study proposed an analytical framework aims at revealing the travel hotspots, their spatial autocorrelation, and the community structure characteristics through the graph-based approach and complex network theory. The main conclusions are as follows.

1. Penn Station and Grand Central Terminal are hotspots for taxis at any peak times of the day. When traveling for commuting, the destinations for passengers in the morning rush hours are concentrated in many financial and commercial areas of Manhattan, while are widely distributed in more diverse places in the evening. When traveling for entertainment, the hotspots for taxi rides during the daytime are concentrated in large department stores, parks, and churches, whereas people are more willing to arrive at theaters at night. Travel demand in NYC shows a strong positive spatial autocorrelation during multiple peak times. In the meanwhile, taxis are more inclined to carry passengers in central Manhattan and transport passengers to peripheral areas.

2. Over different rush hours, the movement of taxis will form a relatively stable, geographically clustered community structure. After empirical analysis of NYC through weighted distribution and interaction intensity, we found several interesting phenomena: a) Every community exists a very small number of TZs are undertake a large amount of passenger travel activities. Moreover, if the numerical interval is used for statistics, the weighted degree of TZs in the community follows the power-law distribution. b) As the weighted degree of TZs increases, the interaction intensity with the community where they are located first strengthens, then stabilizes, and finally weakens, which is probably due to the lack of land use functions in other neighboring communities. In other words, the formation of a community is determined by the key TZs with numerous passengers, but these TZs may have limited connection with the community in which they are located.

Although taxis can reflect residents' travel behavior, there is an inherent sampling deviation, because not all urban residents choose taxis as their travel mode. Future work will improve this problem and extend the analysis to a longer time span to understand the spatiotemporal pattern and the mechanism of the community structure evolution. It can also be further studied in combination with land use data to obtain more refined results.

Acknowledgments

The authors thank OSM contributors for providing the map data. The authors appreciate reviewers and the editor for their insightful comments and suggestions of this work.

Author Contributions

Data curation: Chen Xie.

Formal analysis: Chen Xie, Xiaoyu Zheng.

Funding acquisition: Dexin Yu.

Methodology: Chen Xie.

Supervision: Dexin Yu.

Visualization: Xiaoyu Zheng.

Writing – original draft: Chen Xie.

Writing – review & editing: Zhuorui Wang, Zhongtai Jiang.

References

1. Zhong C, Arisona SM, Huang X, Batty M, Schmitt G. Detecting the dynamics of urban structure through spatial network analysis. International Journal of Geographical Information Science. 2014; 28: 2178–2199. https://doi.org/10.1080/13658816.2014.914521
2. Yang Y, Heppenstall A, Turner A, Comber A. A spatiotemporal and graph-based analysis of dockless bike sharing patterns to understand urban flows over the last mile. Computers, Environment and Urban Systems. 2019; 77: 101361. https://doi.org/10.1016/j.compenvurbsys.2019.101361
3. Barr LC. Testing for the Significance of Induced Highway Travel Demand in Metropolitan Areas. Transportation Research Record. 2000; 1706: 1–8. https://doi.org/10.3141/1706-01
4. Egu O, Bonnel P. How comparable are origin-destination matrices estimated from automatic fare collection, origin-destination surveys and household travel survey? An empirical investigation in Lyon. Transportation Research Part A: Policy and Practice. 2020; 138: 267–282. https://doi.org/10.1016/j.tra.2020.05.021
5. Jin S, Yang J, Wang E, Liu J. The influence of high-speed rail on ice–snow tourism in northeastern China. Tourism Management. 2020; 78: 104070. https://doi.org/10.1016/j.tourman.2019.104070
6. Munizaga MA, Palma C. Estimation of a disaggregate multimodal public transport Origin–Destination matrix from passive smartcard data from Santiago, Chile. Transportation Research Part C: Emerging Technologies. 2012; 24: 9–18. https://doi.org/10.1016/j.trc.2012.01.007
7. Park JY, Kim D-J, Lim Y. Use of Smart Card Data to Define Public Transit Use in Seoul, South Korea. Transportation Research Record. 2008; 2063: 3–9. https://doi.org/10.3141/2063-01
8. Yang C, Yan F, Ukkusuri SV. Unraveling traveler mobility patterns and predicting user behavior in the Shenzhen metro system. Transportmetrica A: Transport Science. 2018; 14: 576–597. https://doi.org/10.1080/23249935.2017.1412370
9. Wang M, Yang S, Sun Y, Gao J. Human mobility prediction from region functions with taxi trajectories. Ma X, editor. PLoS ONE. 2017; 12: e0188735. https://doi.org/10.1371/journal.pone.0188735 PMID: 29190708
10. Widhalm P, Yang Y, Ulm M, Athavale S, González MC. Discovering urban activity patterns in cell phone data. Transportation. 2015; 42: 597–623. https://doi.org/10.1007/s11116-015-9598-x
11. Yu D, Li Z. Study on Users' Travel Behavior of Urban Car Sharing System Based on Spatio-temporal Big Data in Chengdu. J Phys: Conf Ser. 2021; 1910: 012046. https://doi.org/10.1088/1742-6596/1910/1/012046
12. Cai H, Jia X, Chiu ASF, Hu X, Xu M. Siting public electric vehicle charging stations in Beijing using big-data informed travel patterns of the taxi fleet. Transportation Research Part D: Transport and Environment. 2014; 33: 39–46. https://doi.org/10.1016/j.trd.2014.09.003
13. Zhang D, Zhou C, Sun D, Qian Y. The influence of the spatial pattern of urban road networks on the quality of business environments: the case of Dalian City. Environ Dev Sustain. 2021 [cited 13 Oct 2021]. https://doi.org/10.1007/s10668-021-01832-z
14. Liu L, Jiang C, Zhou S, Liu K, Du F. Impact of public bus system on spatial burglary patterns in a Chinese urban context. Applied Geography. 2017; 89: 142–149. https://doi.org/10.1016/j.apgeog.2017.11.002
15. Song J, Zhang L, Qin Z, Ramli MA. A spatiotemporal dynamic analyses approach for dockless bike-share system. Computers, Environment and Urban Systems. 2021; 85: 101566. https://doi.org/10.1016/j.compenvurbsys.2020.101566
16. Gao J, Xie K, Ozbay K. Exploring the Spatial Dependence and Selection Bias of Double Parking Citations Data. Transportation Research Record. 2018; 2672: 159–169. https://doi.org/10.1177/0361198118792323
17. Zhang L, Meng Q, Fang Fwa T. Big AIS data based spatial-temporal analyses of ship traffic in Singapore port waters. Transportation Research Part E: Logistics and Transportation Review. 2019; 129: 287–304. https://doi.org/10.1016/j.tre.2017.07.011
18. Barthélemy M, Flammini A. Modeling Urban Street Patterns. Phys Rev Lett. 2008; 100: 138702. https://doi.org/10.1103/PhysRevLett.100.138702 PMID: 18518005

19. Dhanani A, Tarkhanyan L, Vaughan L. Estimating pedestrian demand for active transport evaluation and planning. Transportation Research Part A: Policy and Practice. 2017; 103: 54–69. https://doi.org/10.1016/j.tra.2017.05.020

20. Yildirimoglu M, Kim J. Identification of communities in urban mobility networks using multi-layer graphs of network traffic. Transportation Research Part C: Emerging Technologies. 2018; 89: 254–267. https://doi.org/10.1016/j.trc.2018.02.015

21. Sun L. Community structure in traffic zones based on travel demand. Physica A. 2016; 8.

22. de Arruda HF, Comin CH, da Fontoura Costa L. Minimal paths between communities induced by geographical networks. J Stat Mech. 2016; 2016: 023403. https://doi.org/10.1088/1742-5468/2016/02/023403

23. Zhang H, Zhang L, Che F, Jia J, Shi B. Revealing Urban Traffic Demand by Constructing Dynamic Networks With Taxi Trajectory Data. IEEE Access. 2020; 8: 147673–147681. https://doi.org/10.1109/ACCESS.2020.3015752

24. Liu FT, Ting KM, Zhou Z-H. Isolation Forest. 2008 Eighth IEEE International Conference on Data Mining. Pisa, Italy: IEEE; 2008. pp. 413–422. https://doi.org/10.1109/ICDM.2008.17

25. Louail T, Lenormand M, Cantu Ros OG, Picornell M, Herranz R, Frias-Martinez E, et al. From mobile phone data to the spatial structure of cities. Sci Rep. 2015; 4: 5276. https://doi.org/10.1038/srep05276 PMID: 24923248

26. Al-Aamri AK, Hornby G, Zhang L-C, Al-Maniri AA, Padmadas SS. Mapping road traffic crash hotspots using GIS-based methods: A case study of Muscat Governorate in the Sultanate of Oman. Spatial Statistics. 2021; 42: 100458. https://doi.org/10.1016/j.spasta.2020.100458

27. Le KG, Liu P, Lin L-T. Traffic accident hotspot identification by integrating kernel density estimation and spatial autocorrelation analysis: a case study. International Journal of Crashworthiness. 2020; 1–11. https://doi.org/10.1080/13588265.2020.1826800

28. Zhou C, Zhang D, He X. Transportation Accessibility Evaluation of Educational Institutions Conducting Field Environmental Education Activities in Ecological Protection Areas: A Case Study of Zhuhai City. Sustainability. 2021; 13: 9392. https://doi.org/10.3390/su13169392

29. Silverman BW. Density Estimation for Statistics and Data Analysis. CRC Press; 1986.

30. Anselin L. Local Indicators of Spatial Association-LISA. Geographical Analysis. 2010; 27: 93–115. https://doi.org/10.1111/j.1538-4632.1995.tb00338.x

31. Blondel VD, Guillaume J-L, Lambiotte R, Lefebvre E. Fast unfolding of communities in large networks. J Stat Mech. 2008; 2008: P10008. https://doi.org/10.1088/1742-5468/2008/10/P10008

32. Barrat A, Barthelemy M, Pastor-Satorras R, Vespignani A. The architecture of complex weighted networks. Proceedings of the National Academy of Sciences. 2004; 101: 3747–3752. https://doi.org/10.1073/pnas.0400087101 PMID: 15007165

33. Newman MEJ. Analysis of weighted networks. Phys Rev E. 2004; 70: 056131. https://doi.org/10.1103/PhysRevE.70.056131 PMID: 15600716

34. Opsahl T, Agneessens F, Skvoretz J. Node centrality in weighted networks: Generalizing degree and shortest paths. Social Networks. 2010; 32: 245–251. https://doi.org/10.1016/j.socnet.2010.03.006

35. Albert R, Barabasi A-L. Statistical mechanics of complex networks. Rev Mod Phys. 2002; 74: 47–97. https://doi.org/10.1103/RevModPhys.74.47

36. Yang J, Yang R, Chen M-H, Su C-H (Joan), Zhi Y, Xi J. Effects of rural revitalization on rural tourism. Journal of Hospitality and Tourism Management. 2021; 47: 35–45. https://doi.org/10.1016/j.jhtm.2021.02.008

37. Ewing RH, Bartholomew K. Best practices in metropolitan transportation planning. London: New York: Routledge, Taylor and Francis Group; 2018.

38. Li Y, Xiong W, Wang X. Does polycentric and compact development alleviate urban traffic congestion? A case study of 98 Chinese cities. Cities. 2019; 88: 100–111. https://doi.org/10.1016/j.cities.2019.01.017

39. Ewing R, Tian G, Lyons T. Does compact development increase or reduce traffic congestion? Cities. 2018; 72: 94–101. https://doi.org/10.1016/j.cities.2017.08.010

40. Sun H, Zhang H, Wu J. Correlated scale-free network with community: modeling and transportation dynamics. Nonlinear Dyn. 2012; 69: 2097–2104. https://doi.org/10.1007/s11071-012-0411-5